Spectrochimica Acta Part B 63 (2008) 1268–1273

Contents lists available at ScienceDirect

Spectrochimica Acta Part B

journal homepage: www.elsevier.com/locate/sab

A new detection system for laser induced breakdown spectroscopy based on an acousto-optical tunable filter coupled to a photomultiplier: Application for manganese determination in steel

Fabiano Barbieri Gonzaga *, Celio Pasquini

Chemistry Institute/P.O. Box 6154, University of Campinas–UNICAMP, 13084-971, Campinas, SP, Brazil

ARTICLE INFO

Article history:
Received 20 June 2008
Accepted 17 September 2008
Available online 6 October 2008

Keywords:
LIBS
Detection system
AOTF
Mn determination

ABSTRACT

The development of a new detection system for laser induced breakdown spectroscopy (LIBS), based on a collinear quartz acousto-optical tunable filter (AOTF) for the ultraviolet spectral region coupled to a photomultiplier, is described. It was used in conjunction with a 1064 nm, 5 ns pulse duration neodymium-doped yttrium aluminium garnet (Nd:YAG) laser source and also employed a radio-frequency signal generator to control the AOTF and a digital delay generator to delay the start of the detection in relation to the instant of the application of the laser pulse. The detection system was optimized for highest detectivity for the manganese peak at 293.9 nm while analyzing a steel sample by LIBS. The resulting signal to background ratio at the optimal conditions of 2 μs delay time, 40 μs integration time gate and 110 mJ pulse energy was similar to that of a commercial echelle-intensified charge-coupled device (echelle-ICCD) detection system. The new detection system was then employed for manganese determination in steel samples, taking the emission signals at just 15 wavelengths, 5 related to the above mentioned manganese peak, another 5 to background emission around 296.0 nm and the others to the iron peak at 297.3 nm (internal standard). The resulting analytical curve for manganese, obtained using 5 samples in the concentration range of 0.214 to 0.939% w/w, presented a correlation coefficient of 0.979 for an exponential regression function. The relative errors of predicting the manganese concentrations, using the calibration curve, for 2 samples, containing 0.277 and 0.608% w/w, were 20.7 and −1.9%, respectively.

1. Introduction

Laser induced breakdown spectroscopy (LIBS) is an analytical technique based on the application of one or more high power short duration laser pulses on a restricted region of the sample to be analyzed, promoting its ablation and/or excitation, with the formation of a transient plasma, whose emitted radiation is monitored by means of an appropriate detection system (wavelength selector and detector) and which is associated with the chemical composition of the sample [1,2].

In recent decades, the development of modern solid state lasers (more compact and with shorter pulse duration), high resolution and wide spectral coverage polychromators, and highly sensitive gated detectors have contributed to the increase of interest in LIBS. Nowadays, common LIBS instrumentation includes, in addition to the laser source, an optical system to drive and focus the laser radiation onto the sample and to collect the radiation emitted by the plasma, a wavelength selector, such as an optical filter [3] or a grating polychromator, and a detector, such as a photomultiplier (PMT) [4,5] (used to monitor discrete wavelengths) or a solid state sensor array. Several reviews about this promising analytical technique, including its instrumentation, have been published in recent years [1,6–12]. Recently, the use of a special kind of grating polychromator, called an echelle polychromator, associated with an intensified charge coupled device containing a bi-dimensional sensor array (ICCD camera) has increased in LIBS due to its high resolution, high sensitivity and gating capabilities [13–19]. However, as the instrumental components of this special detection system are very expensive and their dimensions impede their integration into portable instruments, there is still a need for new detection systems for LIBS, preferably with high resolution and high detectivity.

One of the interesting fields of LIBS applications has been in the metallurgical industry, due to the need for fast and direct analysis of products, saving time and operating costs. Among the most analyzed samples, such as brass [20], gold [21], copper [22,23] and aluminum alloys [24,25], steel accounts for most LIBS applications [26–29], probably due to its wide industrial applications. In steel-making processes, some added elements, such as manganese, play an important role for improving mechanical and chemical properties, such as strength, toughness and heat and corrosion resistance. Thus,

* Corresponding author. Tel.: +55 19 3521 3037; fax: +55 19 3521 3023.
E-mail address: fbgalo@gmail.com (F.B. Gonzaga).

0584-8547/$ – see front matter © 2008 Elsevier B.V. All rights reserved.
doi:10.1016/j.sab.2008.09.014

the manganese content must be strictly controlled, since it contributes to determining the performance of steel materials, and a rapid and precise analytical method would be desirable [30]. Although other well-established atomic emission spectroscopic techniques, such as ICP OES, commonly have lower limits of detection and better accuracy and reproducibility than LIBS for elemental determinations, LIBS presents important advantages for fast and direct analysis of practically any kind of sample, due to its practically non-destructive feature, the possibility of micro-analysis, and other characteristics [1], making it a very attractive tool for the metallurgical industry.

Unlike dispersive polychromators, optical filters are less employed as wavelength selectors in LIBS mainly because of their lower resolution and the selection of usually just one wavelength band at their exit, limiting the number of emission lines that can be simultaneously detected to one line per filter and, therefore, reducing the capability of simultaneous multielement detection. However, due to the higher throughput of optical filters (there is no slit) in relation to dispersive spectrographs, modern tunable filters, such as acousto-optical tunable filters (AOTF), have been used in LIBS for plasma imaging, at a particular line emission, using a bi-dimensional sensor array [3,31–33]. An AOTF is an optical band pass filter based on the diffraction of the radiation by an acoustic wave, whose frequency determines the selected wavelength, propagating through an isotropic or anisotropic crystal medium (the material the AOTF is made of) [34,35]. The advantages of the AOTF and its applications in analytical spectrometry has been described and reviewed elsewhere [35,36]. It presents a high energy throughput, fast wavelength switching capability and robustness (no-moving parts), providing a simple optical design for a detection system at several wavelength ranges (from ultraviolet to mid-infrared). As the lower the wavelength range, the higher the resolution of AOTF, the use of an AOTF for the ultraviolet spectral range coupled to a modern photomultiplier module, with gating capabilities, can provide a new high resolution and high sensitivity detection system for LIBS.

To the best of our knowledge, the use of AOTF as a wavelength selector for LIBS together with its analytical application for quantitative determination has not been described. Thus, the present paper describes a new detection system for LIBS, based on a collinear quartz AOTF for the ultraviolet spectral region coupled to a photomultiplier module, and its use for manganese determination on steel.

2. Experimental section

2.1. Instrumentation

The laser source employed was an actively Q-switched Nd:YAG laser (Quantel Brilliant) with 1064 nm wavelength, 360 mJ pulse energy, 5 ns pulse duration and 20 Hz pulse repetition rate. The laser pulses were driven and focused onto the sample surface using a dichroic mirror and a BK7 biconvex lens. The lens position was adjusted so that its focus (25 cm) was located 0.5 cm below the sample surface. The emitted radiation of the plasma was collected by means of a quartz bi-convex lens (short focal length), placed at 45° in relation to the sample surface and coupled to an optical fiber bundle (2.4 mm active diameter) that was connected to the entrance of the home-made detection system. The detection system was composed basically of a quartz plane-convex collimating lens (3.8 cm focus), two α-BBO (barium borate) Glan Thompson polarizers, a quartz collinear AOTF covering the spectral range from 250 to 400 nm (Brimrose QZAF5-0.25-0.4) and a photomultiplier module (Hamamatsu H7468-03). The polarizers were placed, in a crossed configuration, in front of the entrance and the exit windows of the AOTF, with the first order beam being selected by 90° polarization rotation inside the AOTF and the zero order beam being extinguished by the polarizers. A schematic representation of that instrumental setup is shown on Fig. 1. The system also employed a radio-frequency (rf) signal generator (Brimrose VFI122.5-85-PPS B2-C12) to control the AOTF and a digital

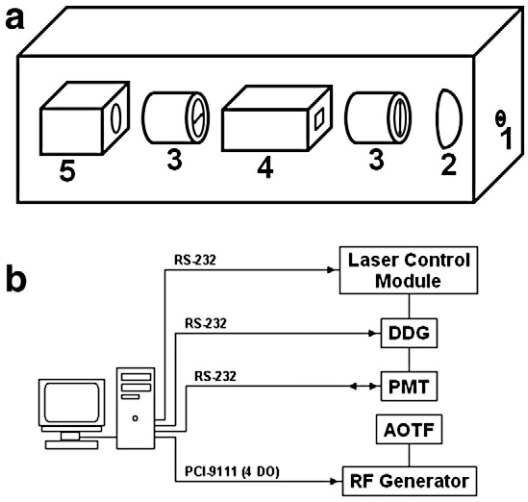

Fig. 1. (a) Scheme of the new detection system: (1) entrance connector of the optical fiber bundle, (2) quartz plane-convex collimating lens, (3) Glan Thompson polarizers, (4) AOTF, (5) photomultiplier module; (b) scheme of control and data acquisition connections.

delay generator (DDG – Highland Technology T550) to delay the start of the detection in relation to the application of the laser pulse. The calibration between the rf signal applied to the AOTF and the resulting wavelength selected by it was made using a Hg/Ar calibration source (Ocean Optics HG-1). A microcomputer containing a communication interface (ADLink PCI-9111) and running home-made software (developed in Microsoft Visual Basic .Net 2003) was used to control the laser source, the DDG and the rf generator and for data acquisition from the photomultiplier module, as shown of Fig. 2. For comparison purposes, a commercial detection system having an echelle spectrograph (Andor Mechelle ME 5000) coupled to a 1024×1024 pixel intensified charge coupled device (ICCD) camera (Andor iStar DH734-18F-03) was also employed. In this latter case, another optical fiber cable (50 μm core diameter), connected to the entrance of the echelle spectrograph, was used to collect the plasma radiation.

2.2. Samples

7 steel samples with manganese contents from 0.214 to 0.939% w/w were analyzed by LIBS using the home-made detection system. The samples were secondary standard materials, since the manganese concentrations had been previously determined by ICP OES, to show average standard deviation of the Mn concentrations of 0.008%, evaluated by analyzing five replicates of three samples with different concentration levels. In addition, a copper foil sample was also analyzed in the preliminary evaluation of the detection system.

2.3. Experimental procedure for manganese determination

The samples were pre-treated by polishing in order to remove surface contamination. Every steel sample was analyzed in 5 replicates, each applying the laser pulses at a different surface location. Each laser pulse had 110 mJ energy (adjusted by varying the laser Q-switch delay), giving a theoretical irradiance of about 4.1×10^{10} W cm^{-2} pulse^{-1} and a theoretical spot size of about 5.4×10^{-4} cm^2, calculated according to the literature [37]. The emission intensities were taken at 15 different pre-selected wavelengths covering 3 narrow spectral ranges: 5 wavelengths around 293.9 (a manganese peak), 5 around 296.0 (baseline) and 5 around 297.3 nm (an iron peak as reference). The detection was gated using 2 μs of delay time and 40 μs of integration time gate. As the AOTF is a monochromator, just one emission intensity could be taken at a specific wavelength for each laser pulse. Therefore, for each replicate, 150 laser pulses were applied in order to allow 10 emission

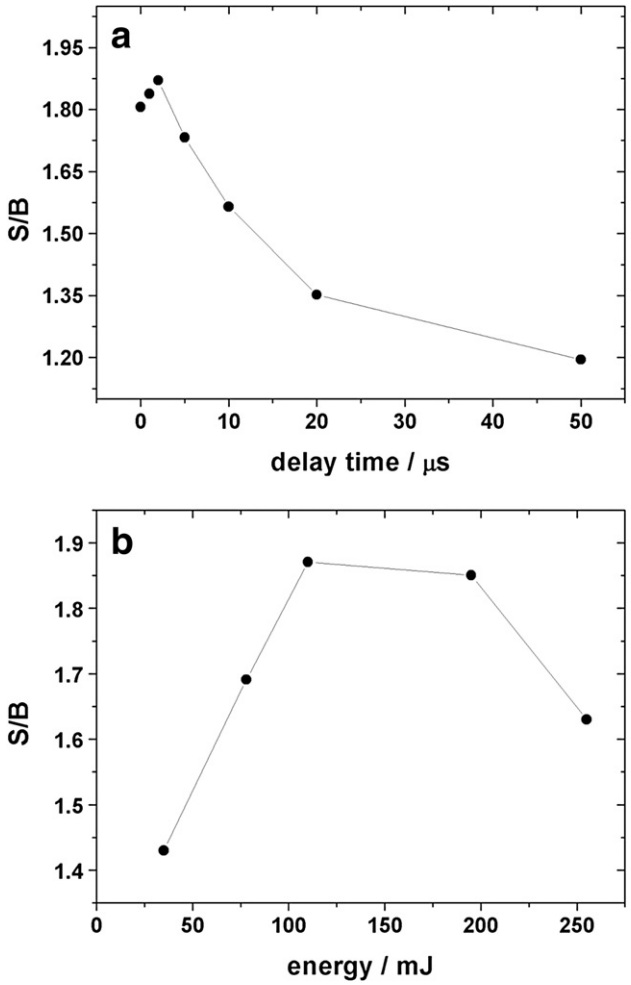

Fig. 2. Variation of the S/B value of the manganese emission peak according to (a) the delay time and (b) the laser pulse energy employed.

measurements at each wavelength. The 50 measurements for each wavelength were averaged and the 15 resulting values were integrated within each narrow spectral range, giving just 3 emission measurements per sample. Finally, the analytical signal was calculated by normalizing the result related to 293.9 nm against the result related to 297.3 nm (discussed later). The analytical signals of 5 samples were employed for the construction of an analytical curve for manganese concentration. The analytical signals of the remaining 2 samples were employed for predicting their manganese concentrations using the analytical curve. These last 2 samples were analyzed three times, repeating the above procedure, in order to obtain the standard deviations of the determinations.

3. Results and discussion

3.1. Evaluation and optimization

For the preliminary evaluation of the proposed detection system and for the optimization of the analytical parameters, one of the steel samples was chosen and analyzed and the manganese emission peak at 293.9 nm was studied in terms of signal to background ratio (S/B), full width at half maximum (FWHM) and relative standard deviation at maximum (RSD). A LIBS spectrum of this steel sample, acquired with the home-made detection system and containing the mentioned emission peak, is shown in Fig. 3a. For obtaining the spectrum, one laser pulse has to be applied for each emission signal to be acquired at each wavelength. In addition, this spectrum was an average of 50 spectra, every 10 taken at one of 5 different locations. However, in order to evaluate the S/B and the RSD, wavelength scanning was not necessary, since measurements can be made at discrete wavelengths using the AOTF, similar to the procedure described in the previous section. The S/B value was calculated for each location (after averaging the 10 measurements for each wavelength) by rationing the peak intensity (highest value) by the average background (5 values around 296 nm). Then, the final S/B value was the average of the S/B values for the different locations. The RSD was calculated using the peak intensity of the 50 measurements and the FWHM was calculated using the acquired spectra.

Firstly, the delay time was varied from 0 to 50 μs, together with the increase of the gain of the photomultiplier (as high as possible without saturating its signal), and the S/B and RSD were evaluated. The pulse energy was initially kept at a moderate value (110 mJ) and the integration time gate used was 40 μs for all this work (minimum value supported by the photomultiplier). This study was necessary because it was not possible to use high gain values of the photomultiplier without saturating its signal when non-gated detection was employed. A decrease in the background signal was observed up to 2 μs of delay time, while keeping the peak intensity, resulting in an increasing S/B value, as shown on Fig. 2a. The RSD did not vary significantly along the delay time range studied, always being lower than 8%. Therefore, a delay time of 2 μs was chosen to be used in the remainder of this work.

The second parameter optimized was the laser pulse energy. For that, similar to the delay time study, the pulse energy was varied

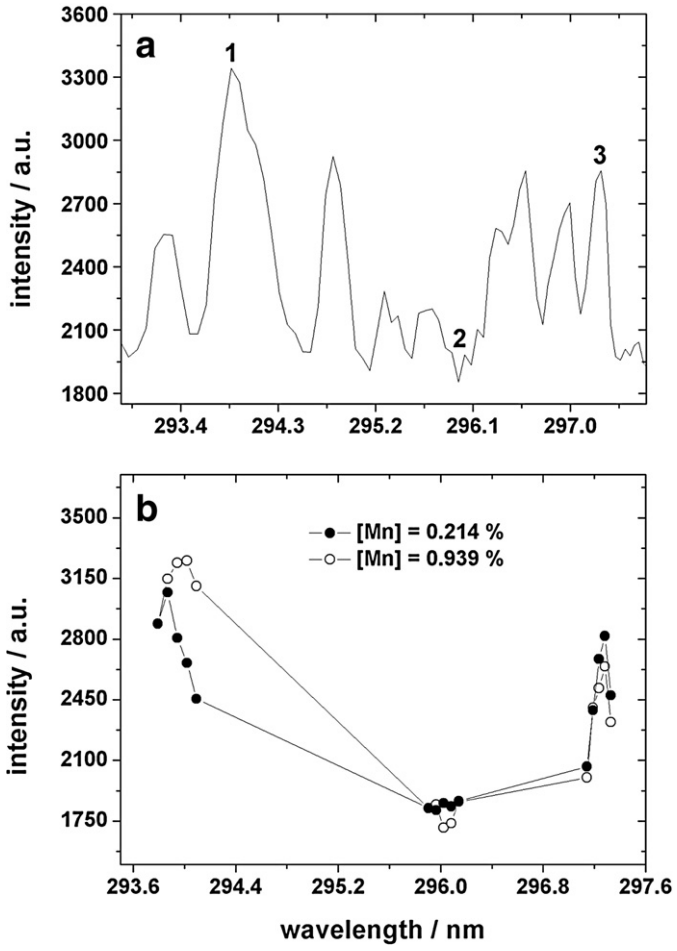

Fig. 3. (a) LIBS spectra of a steel sample in the spectral range used for manganese determination: (1) manganese peak, (2) background, (3) iron peak; (b) LIBS emission signals taken at just 15 wavelengths for two steel samples having different manganese concentrations.

from 255 to 25 mJ (by continuously increasing the laser Q-switch delay), in conjunction with the increase of the gain of the photomultiplier, and the S/B and RSD were evaluated. The result was a maximum S/B value at 110 mJ, as shown on Fig. 2b. The RSD did not vary significantly along the energy range studied, always being lower than 8%. Thus, a pulse energy of 110 mJ was chosen to be used in the remainder of this work.

At this point, the performance of the home-made detection system was compared to that of a commercial echelle-ICCD-based detection system, commonly used in LIBS, using the same analytical parameters. Both were compared in terms of S/B, FWHM and RSD for the mentioned manganese peak. For the echelle-ICCD-based detection system, a moderate gain (150 of up to 255) was employed in the microchannel plate. In addition, a procedure similar to that used for the home-made detection system was employed: 10 spectra were acquired for each of the 5 locations, resulting in 50 spectra. The results are shown in the first two lines of Table 1. As can be seen, both detection systems had similar performances in terms of sensitivity. However, the echelle-ICCD-based detection system presented a better spectral resolution (lower FWHM value), as expected due to the high resolution of the echelle spectrograph, while the home-made detection system presented a better signal repeatability (lower RSD value).

In order to evaluate the real gain of using the 2.4 mm optical fiber cable for LIBS measurements (taking advantage of the wide windows of the AOTF and the photomultiplier), the home-made detection system was also evaluated using the 50 µm optical fiber cable (the same used for the echelle-ICCD-based detection system). The results are shown in the last line of Table 1. As can be seen, although the 2.4 mm optical fiber cable allowed the collection of more radiation from the plasma, its use did not take to a better sensitivity (in terms of S/B). However, the use of the 50 µm optical fiber cable with the home-made detection system led to a worse repeatability. That can be explained by the use of a higher gain in the photomultiplier when using the 50 µm optical fiber cable and/or by the fact that it is easier to collect the radiation from a wider portion of the plasma when using a bigger optical fiber cable. This last supposition is also supported by the similar RSD values found for the echelle-ICCD-based detection system and for the home-made detection system employing the 50 µm optical fiber cable.

Although the S/B values were relatively low for the mentioned manganese emission peak, for the copper emission peak at 324.7 nm in a copper sample (a majority component in a simpler matrix), the S/B values obtained were above 50 for both detection systems, using the optimized conditions of 10 µs delay time and 78 mJ pulse energy.

3.2. Manganese determination

For manganese determination, the spectral region shown in Fig. 3a was chosen as it contains several manganese emission peaks that have already been used for manganese determination in steel using LIBS [29]. Two peaks in the spectrum, one at about 293.9 nm and another at about 297.3 nm, were identified as manganese and iron emission peaks, respectively, and chosen for manganese determination using iron as internal standard. In addition, the emission at about 296.0 nm, between the above mentioned two peaks, was selected for background subtraction. Here, it is important to point out that, although AOTF is a monochromator and the simultaneous acquisition of emission signals in a given spectral range is not possible (as when using polychromators), the acquisition of specific atomic emission signals and the related background emissions is perfectly possible and viable, as shown in Fig. 3, just requiring the application of more laser pulses. It is also important to point out that, in LIBS, the background from subsequent plasma does not necessarily reflect that of the earlier plasma and, therefore, it is notoriously difficult to obtain meaningful spectra by taking background measurements on different plasma than the one used to take the analytical atomic line. In this way, it is very interesting that the approach employed in this work, by generating different plasmas for every measurement to be made at every wavelength, have worked well. We think that occurred not only because the process was reproducible on a pulse to pulse level, but also because of the high number of measurements taken and averaged for each wavelength.

Actually, for the manganese determination, emission signals were taken at 15 different wavelengths, as described in the Experimental section: 5 wavelengths around each selected emission peak and 5 more around the wavelength selected as background emission. This was done to improve signal precision by means of the integration of the emission signals related to the same spectral information. Two sets of 15 emission signals taken at these selected wavelengths for 2 steel samples with very different manganese concentrations are shown in Fig. 3b. As expected, the emission intensities around 393.9 nm were very dependent on the manganese concentrations.

After the experimental measurements were taken (as described in the experimental procedure), several approaches were investigated for the construction of the analytical curve for manganese: (i) direct use of the signals related to the manganese peak, (ii) use of the manganese signals after background subtraction, (iii) the direct ratio of the manganese signals to the respective iron signals and (iv) the ratio of the manganese signals to the respective iron signals after background subtraction of both. In addition, different regression functions were tried to fit the data. The better results, considering both the regression parameters and the prediction of the manganese concentrations, were obtained using the direct ratio of the manganese signals to the respective iron signals and an exponential regression function. The resulting analytical curve is shown in Fig. 4. As background subtraction was not necessary, new steel samples could be analyzed taking measurements at just 10 wavelengths.

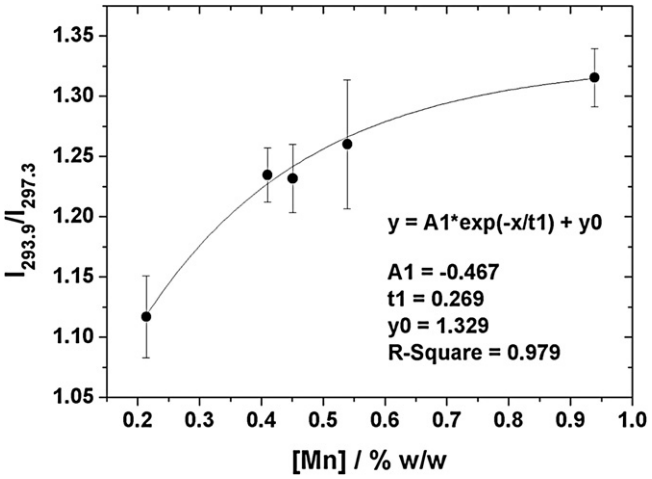

Fig. 4. Calibration curve for manganese concentration in steel.

Table 1
Comparison between the proposed detection system and a commercial echelle-ICCD-based detection system for the manganese peak at 293.9 nm in a steel sample (40 µs integration time gate, 2 µs delay time and 110 mJ pulse energy)

Detection system	S/B	FWHM/nm	RSD/%
Echelle-ICCD[a]	2.03	0.24	15.78
AOTF-PMT[b]	1.87	0.5	10.63
AOTF-PMT[c]	1.98	0.5	15.82

S/B = signal to background ratio.
FWHM = full width at half maximum.
RSD = relative standard deviation between 50 measures.
[a] using a gain of 150 in the microchannel plate.
[b] using a gain related to 410 V applied in the PMT and the 2.4 mm optical fiber cable.
[c] using a gain related to 1000 V applied in the PMT and the 50 µm optical fiber cable.

Table 2
Results of predicting manganese concentrations for 2 steel samples

$[Mn]_{REF}$/% w/w	$[Mn]_{DET}$/% w/w	Error/%
0.277	0.334±0.028	20.7
0.608	0.597±0.151	−1.9

$[Mn]_{REF}$ = manganese concentration determined by the reference method.
$[Mn]_{DET}$ = manganese concentration determined by the present method.

The results for the prediction of the manganese concentrations in 2 steel samples using the analytical curve are shown in Table 2. The result for the less concentrated sample presented a relatively high error in relation to the reference value, which was due to its low manganese concentration, while the result for the high concentrated sample presented a relatively high standard deviation, which can be explained by the decreasing slope of the regression curve as the manganese concentration increases. In addition, the precision found for the manganese prediction was possibly affected by the low number of samples used for the calibration.

The correlation coefficient of the analytical curve and the errors found in the prediction of the manganese concentrations were similar to those commonly obtained for manganese determination in steel, for samples with similar concentration ranges, using LIBS with high resolution dispersive polychromators coupled to gated detectors [29].

4. Conclusions

This paper has described the development of a home-made detection system for LIBS, composed basically of a collinear quartz AOTF for the ultraviolet spectral region coupled to a photomultiplier. The new detection system was successfully applied for manganese determination in steel samples by LIBS, using a Nd:YAG laser source for ablation and excitation.

The performance of the detection system for LIBS, after its optimization for highest detectivity using a manganese peak while analyzing a steel sample, was similar, in terms of sensitivity, and better, in terms of repeatability, to that of a commercial echelle-ICCD-based detection system. The better repeatability was provided by the use of the 2.4 mm optical fiber bundle in conjunction with the wide windows of the AOTF and the photomultiplier.

For manganese determination in steel, although the emission signals were taken at 15 wavelengths, analyses using just 10 wavelengths were possible, 5 related to a manganese peak and 5 to an iron peak. The resulting analytical curve presented a good correlation coefficient and the errors found on predicting the manganese concentrations of 2 samples using the analytical curve were relatively low for LIBS. That demonstrated the good performance of the proposed detection system for quantitative determinations in LIBS.

Although the use of high resolution dispersive polychromators coupled to an intensified gated array of detectors has become almost compulsory in LIBS, the development of alternative detection systems for LIBS, such as that described in this paper, are very important in order to contribute to the dissemination of this analytical technique. In addition, the use of AOTF in LIBS showed to be very attractive because, although AOTF is a monochromator and the simultaneous acquisition of emission signals in a given spectral range is not possible, it has no need for an entrance slit, it is sufficiently compact to be included in portable instruments and, for specific applications where the wavelengths of atomic emissions of interest are already known, it can be used to monitor the emissions at just these wavelengths, thus constituting a very versatile analyzer for LIBS.

Acknowledgements

The authors are grateful to Dr. C. H. Collins for manuscript revision. F. B. G. wishes to thanks FAPESP for a post-doctoral fellowship.

References

[1] C. Pasquini, J. Cortez, L.M.C. Silva, F.B. Gonzaga, Laser induced breakdown spectroscopy, J. Braz. Chem. Soc. 18 (2007) 463–512.
[2] F.B. Gonzaga, C. Pasquini, A complementary metal oxide semiconductor sensor array based detection system for laser induced breakdown spectroscopy: evaluation of calibration strategies and application for manganese determination in steel, Spectrochim. Acta Part B 63 (2008) 56–63.
[3] D.N. Stratis, K.L. Eland, J.C. Carter, S.J. Tomlinson, S.M. Angel, Comparison of acousto-optic and liquid crystal tunable filters for laser-induced breakdown spectroscopy, Appl. Spectrosc. 55 (2001) 999–1004.
[4] R.E. Neuhauser, B. Ferstl, C. Haisch, U. Panne, R. Niessner, Design of a low-cost detection system for laser-induced plasma spectroscopy, Rev. Sci. Instrum. 70 (1999) 3519–3522.
[5] J.S. Huang, C.B. Ke, L.S. Huang, K.C. Lin, The correlation between ion production and emission intensity in the laser-induced breakdown spectroscopy of liquid droplets, Spectrochim. Acta Part B 57 (2002) 35–48.
[6] J. Sneddon, Y. Lee, Novel and recent applications of elemental determination by laser-induced breakdown spectrometry, Anal. Lett. 32 (1999) 2143–2162.
[7] L.J. Radziemski, From LASER to LIBS, the path of technology development, Spectrochim. Acta Part B 57 (2002) 1109–1113.
[8] K. Song, Y. Lee, J. Sneddon, Recent developments in instrumentation for laser induced breakdown spectroscopy, Appl. Spectrosc. Rev. 37 (2002) 89–117.
[9] E. Tognoni, V. Palleschi, M. Corsi, G. Cristoforetti, Quantitative micro-analysis by laser-induced breakdown spectroscopy: a review of the experimental approaches, Spectrochim. Acta Part B 57 (2002) 1115–1130.
[10] J.D. Winefordner, I.B. Gornushkin, T. Correll, E. Gibb, B.W. Smith, N. Omenetto, Comparing several atomic spectrometric methods to the super stars: special emphasis on laser induced breakdown spectrometry, LIBS, a future super star, J. Anal. At. Spectrom. 19 (2004) 1061–1083.
[11] J.M. Vadillo, J.J. Laserna, Laser-induced plasma spectrometry: truly a surface analytical tool, Spectrochim. Acta Part B 59 (2004) 147–161.
[12] K. Song, Y. Lee, J. Sneddon, Applications of laser-induced breakdown spectrometry, Appl. Spectrosc. Rev. 32 (1997) 183–235.
[13] G.R. Harrison, The production of diffraction gratings. 2. the design of echelle gratings and spectrographs, J. Opt. Soc. Am. 39 (1949) 522–528.
[14] C. Haisch, U. Panne, R. Niessner, Combination of an intensified charge coupled device with an echelle spectrograph for analysis of colloidal material by laser-induced plasma spectroscopy, Spectrochim. Acta Part B 53 (1998) 1657–1667.
[15] H.E. Bauer, F. Leis, K. Niemax, Laser induced breakdown spectrometry with an echelle spectrometer and intensified charge coupled device detection, Spectrochim. Acta Part B 53 (1998) 1815–1825.
[16] P. Lindblom, New compact echelle spectrographs with multichannel time-resolved recording capabilities, Anal. Chim. Acta 380 (1999) 353–361.
[17] J. Janesick, G. Putnam, Developments and applications of high-performance CCD and CMOS imaging arrays, Annu. Rev. Nucl. Part. Sci. 53 (2003) 263–300.
[18] M. Sabsabi, V. Detalle, M.A. Harith, W. Tawfik, H. Imam, Comparative study of two new commercial echelle spectrometers equipped with intensified CCD for analysis of laser-induced breakdown spectroscopy, Appl. Opt. 42 (2003) 6094–6098.
[19] C. Haisch, H. Becker-Ross, An electron bombardment CCD-camera as detection system for an echelle spectrometer, Spectrochim. Acta Part B 58 (2003) 1351–1357.
[20] G. Galbács, I.B. Gornushkin, B.W. Smith, J.D. Winefordner, Semi-quantitative analysis of binary alloys using laser-induced breakdown spectroscopy and a new calibration approach based on linear correlation, Spectrochim. Acta Part B 56 (2001) 1159–1173.
[21] M. Corsi, G. Cristoforetti, V. Palleschi, A. Salvetti, E. Tognoni, A fast and accurate method for the determination of precious alloys caratage by laser induced plasma spectroscopy, Eur. Phys. J. Part D 13 (2001) 373–377.
[22] M. Sabsabi, P. Cielo, Quantitative-analysis of copper-alloys by laser-produced plasma spectrometry, J. Anal. At. Spectrom. 10 (1995) 643–647.
[23] F. Colao, R. Fantoni, V. Lazic, L. Caneve, A. Giardini, V. Spizzicchino, LIBS as a diagnostic tool during the laser cleaning of copper based alloys: experimental results, J. Anal. At. Spectrom. 19 (2004) 502–504.
[24] M.A. Ismail, H. Imam, A. Elhassan, W.T. Youniss, M.A. Harith, LIBS limit of detection and plasma parameters of some elements in two different metallic matrices, J. Anal. At. Spectrom. 19 (2004) 489–494.
[25] I.V. Cravetchi, M.T. Taschuk, Y.Y. Tsui, Evaluation of femtosecond LIBS for spectrochemical microanalysis of aluminium alloys, Anal. Bioanal. Chem. 385 (2006) 287–294.
[26] H. Balzer, S. Hölters, V. Sturm, R. Noll, Systematic line selection for online coating thickness measurements of galvanised sheet steel using LIBS, Anal. Bioanal. Chem. 385 (2006) 234–239.
[27] V. Sturm, J. Vrenegor, R. Noll, M. Hemmerlin, Bulk analysis of steel samples with surface scale layers by enhanced laser ablation and LIBS analysis of C, P, S, Al, Cr, Cu, Mn and Mo, J. Anal. At. Spectrom. 19 (2004) 451–456.
[28] C. Lopez-Moreno, K. Amponsah-Manager, B.W. Smith, I.B. Gornushkin, N. Omenetto, S. Palanco, J.J. Laserna, J.D. Winefordner, Quantitative analysis of low-alloy steel by microchip laser induced breakdown spectroscopy, J. Anal. At. Spectrom. 20 (2005) 552–556.
[29] K.Y. Yamamoto, D.A. Cremers, L.E. Foster, M.P. Davies, R.D. Harris, Laser-induced breakdown spectroscopy analysis of solids using a long-pulse (150 ns) Q-switched Nd:YAG laser, Appl. Spectrosc. 59 (2005) 1082–1097.
[30] K. Wagatsuma, K. Kodama, H. Park, Precise determination of manganese in steel by dc glow discharge optical emission spectrometry associated with voltage modulation technique, Anal. Chim. Acta 502 (2004) 257–263.
[31] R.A. Multari, L.E. Foster, D.A. Cremers, M.J. Ferris, Effect of sampling geometry on elemental emissions in laser-induced breakdown spectroscopy, Appl. Spectrosc. 50 (1996) 1483–1499.

[32] R.A. Multari, D.A. Cremers, A time-resolved imaging study of Cr (I) emissions from a laser plasma formed on a sample at nonnormal incidence, IEEE Trans. Plasma Sci. 24 (1996) 39–40.
[33] A.K. Knight, N.L. Scherbarth, D.A. Cremers, M.J. Ferris, Characterization of laser-induced breakdown spectroscopy (LIBS) for application to space exploration, Appl. Spectrosc. 54 (2000) 331–340.
[34] F.B. Gonzaga, C. Pasquini, Near-infrared emission spectrometry based on an acousto-optical tunable filter, Anal. Chem. 77 (2005) 1046–1054.
[35] C.D. Tran, Acoustooptic devices — optical-elements for spectroscopy, Anal. Chem. 64 (1992) 971A–981A.
[36] L. Bei, G.I. Dennis, H.M. Miller, T.W. Spaine, J.W. Carnahan, Acousto-optic tunable filters: fundamentals and applications as applied to chemical analysis techniques, Prog. Quantum Electron. 28 (2004) 67–87.
[37] R. Noll, Terms and notations for laser-induced breakdown spectroscopy, Anal. Bioanal. Chem. 385 (2006) 214–218.